Calcium-mediated Changes in Gap Junction Structure: Evidence from the Low Angle X-ray Pattern

P. N. T. UNWIN and P. D. ENNIS
Department of Structural Biology, Stanford University School of Medicine, Stanford, California 94305

ABSTRACT Rat liver gap junctions were isolated in Ca^{2+}-free media and analyzed in controlled environments by x-ray diffraction of partially oriented pellets. Different treatments of the same preparations were compared. The ordered hexagonal lattices gave rise to detail that was sensitive to low Ca^{2+} concentrations (0.05 mM), but not to Mg^{2+} (up to 0.16 mM) or pH (between 6.0 and 8.0). The major Ca^{2+}-mediated responses were reductions in the intensity of the (1, 0) peak and in the off-equatorial contributions to the (2, 1) peak, and changes of scale equivalent to a decrease (~2%) in lattice dimension, but an increase (~4%) in the dimension perpendicular to the lattice. A simple structural interpretation of these findings is that Ca^{2+} induces the subunits of the channel-forming assembly, the connexon, to align more nearly parallel to the channel, thereby causing the connexon to become slightly longer and more radially compact. The rearrangement is of the same nature as one found under less physiological circumstances by electron microscopy (Unwin, P. N. T., and G. Zampighi, 1980, *Nature (Lond.)*, 283:545–549), and may be part of a coordinated mechanism by which the channel closes.

The gap junction is a region of contact between neighboring animal cells that allows the exchange of small molecules and ions between their interiors (4, 6). The channels responsible for this exchange lie along the hexad axes of hexameric membrane proteins called connexons (2), which link, in pairs, the apposed plasma membranes. In living tissue the connexon responds to local changes in intracellular free Ca^{2+} concentration (10, 11), and/or pH (11, 13) and membrane potential (3, 9), thereby regulating the channel's permeability. The mechanism of the transition between the open and closed states of the channel is not known. However, studies of isolated, hexagonally ordered, gap junctions suggest it may involve a change in conformation of the connexon in the space between the two plasma membranes (1, 7) or, alternatively, a coordinated rearrangement of the connexon subunits around the channel (14).

As a first step toward understanding the physiological significance of these connexon configurations, we examined the structural response of isolated junctions to changes in ionic environment. Response was assessed quantitatively by dividing each preparation in two, exposing the separate portions to different solutions, and then comparing x-ray diffraction patterns recorded from each portion. Pair-wise analysis provided a sensitive measure of structural state, making the effect of small variabilities between preparations relatively unimportant.

Results showed that the isolated junctions change their structure on exposure to low Ca^{2+} concentrations. We report on the properties of this transition, its relation to one previously described (14), and its possible relevance to living tissue.

MATERIALS AND METHODS

Chemicals: Lubrol WX and Arsenazo III were obtained from Sigma Chemical Co. (St. Louis, MO); sodium deoxycholate from Calbiochem-Behring Corp. (La Jolla, CA); and H^3-labeled sodium deoxycholate (4 Ci/mmol) from New England Nuclear (Boston, MA). Sucrose gradients were made using ultrapure sucrose from Schwartz/Mann (Orangeburg, NY). All other chemicals were reagent grade. All solutions were made up with doubled distilled water.

Isolation: The isolation procedure was similar to that described in reference 15. We used 20–30 rats (Sprague-Dawley, Madison, WI), of ~160 g body wt, for each set of experiments. Following excision, their livers (total wet weight: 150–180 g) were pooled and washed in saline. They were transferred to Medium A (0.5 mM EGTA, 1 mM $MgCl_2$, 50 μM phenylmethylsulphonyl fluoride, 4% [wt/wt] sucrose, 10 mM sodium bicarbonate, pH 8.0), cut into small pieces, and homogenized in 20-ml portions in a Potter-Elvehjem glass homogenizer with a loose-fitting teflon pestle. The homogenate was pooled, diluted with Medium A to 4 l, and left to stand for 10 min. It was then filtered two times through four layers of surgical gauze and subsequently through two layers of nylon mesh having 50-μm pores. The filtered homogenate was centrifuged at 4,000 rpm for 20 min (JA-10 rotor, Beckman Instruments, Inc., Palo Alto, CA) and the supernatant was discarded. The top, slightly pink layers of the pellets were collected, pooled, and homogenized using a tight-fitting pestle. The resulting 80-ml suspension was brought to a sucrose concentration of 43% (wt/wt) with 60% (wt/wt) sucrose in Medium A, and adjusted to pH

THE JOURNAL OF CELL BIOLOGY · VOLUME 97 NOVEMBER 1983 1459–1466

8.0; the gravitational densities were monitored with a refractometer (Bausch & Lomb Inc., Rochester, NY). Portions of ~15 ml were transferred to tubes for the Beckman SW27 rotor, equal volumes of Medium A were layered on top, and the tubes were centrifuged at 25,000 rpm for 90 min. The compact white material that migrated to the interfaces was collected, homogenized, diluted with ~200 ml of Medium A, and then centrifuged at 10,000 rpm (Beckman JA-14 rotor) for 10 min. The pellet thus obtained showed a white upper layer and an underlying more yellow zone. The upper layer was carefully resuspended in ~40 ml of Medium A and the sucrose concentration was increased, as before, to 41%. The steps following the sucrose addition were repeated as above, leading to a second pellet, more homogeneous than the first. This pellet was resuspended in a small volume of Medium A and brought to 41% sucrose. The steps following sucrose addition were then repeated a third time, yielding a third pellet, without the underlying yellow zone. The steps subsequent to the production of this third (membrane) pellet, including solubilization in 2% sodium deoxycholate, centrifugation, and resuspension in 0.1% Lubrol WX, were carried out as described (15). The final sucrose density gradient step previously used was replaced by a 5-min 1,500 *g* spin (model 59 microfuge, Fisher Scientific Co., Pittsburg, PA) to remove large aggregates. The resulting gap junction suspension (~0.5 mg of protein) contained a significant proportion of amorphous and fibrous material, but was of adequate purity for the diffraction experiments. All steps in the isolation and subsequent dialysis were carried out at pH 8.0 (unless otherwise specified) between 0 and 4°C.

Dialysis: Gap junction suspensions were dialyzed against 2 l of solution containing 0.02% sodium azide, using 6.4-mm-diam, 12–14,000-mol-wt cutoff, Spectrapor tubing, presoaked in 5 mM EDTA. Dialysis solutions (Table I) were renewed two times during the 3-d duration of this step. Acid-washed glassware was used in experiments designed to test sensitivity of gap junction structure to divalent cations. The Ca^{2+} concentration during dialysis was in some instances checked independently using the dye, Arsenazo III (12), and shown to be equal to that presumed from the amount originally added to the solution.

On the basis of earlier studies (14, 15) it was possible that residual amounts of sodium deoxycholate retained from the isolation procedure might influence details in the diffraction patterns. We estimated the concentrations before and after dialysis using H^3-labeled sodium deoxycholate. Prior to dialysis the concentration was 0.1–0.2% and afterwards it was 0.0023% (±0.0008 SD, $n = 11$), independent of the composition of the low ionic strength dialysis solution. In the experiments below, except for the series specifically investigating the effect of the dialysis, care was taken to keep the concentration of sodium deoxycholate constant at 0.002–0.003% prior to and during recording of the x-ray patterns.

X-ray Diffraction: Partially oriented gap junction pellets were prepared for x-ray diffraction by centrifugation of suspensions in BEEM bottle-neck embedding capsules (Ted Pella, Inc., Tustin, CA) at 30,000 rpm (Beckman SW60 rotor) for 8 h. The plastic around the pellets was cut on either side of the capsule base to create openings for the x-ray beam. The trimmed pellets were placed in an x-ray wet cell so that the beam direction was parallel to the base of the capsule and hence predominantly parallel to the junction surfaces. The wet cell was maintained at 100% humidity at 5–10°C. X-ray patterns were recorded from the same region of each pellet, ~100 μm from the bottom. Pilot experiments showed these patterns to be stable over the 2–3-d exposure periods, so that fixatives were not used.

The x-ray source was CuKα radiation from an Elliot GX13 rotating anode generator, having a 1.0 mm × 100 μm focal cup. The camera was of the Franks type, incorporating two 6-cm glass mirrors and two collimating slits. The focused spot was sufficiently small, ~100 × 150 μm, that detail in the x-ray patterns was limited by junctional disorder rather than by the beam size. The collimating slits, wet cell, and film cassette were contained within a helium-filled box to minimize air scatter. The positions of the optical elements were fixed. No changes were made to the optical configuration, apart from the minor alignment necessary following filament replacements, throughout the course of experiments. The specimen-to-film distance was 92.0 mm. Errors in measurement of lattice dimension, due to flexure of film within the cassette and small variations in the positioning of the sample within the wet cell, were < 0.3%.

Processing of X-ray Films: Patterns were recorded on CEA reflex film, stacked three sheets thick, and developed in full strength Kodak D19 for 6 min. Films were digitized into 527 × 500 arrays of optical densities using an automatic microdensitometer (Perkin-Elmer Corp., Eden Prairie, MN) with the step size adjusted to 25 μm and a sampling aperture of 25 × 25 μm^2. The optical density values along circular arcs centered on the equator or meridian were integrated and plotted as a function of reciprocal distance, after corrections were made for the geometry of the camera, by using a computer program written by D. Austen (Stanford University). Integrations over sector angles of 30 and 10°, from both sides of the pattern, were used to produce equatorial and meridional traces, respectively. The position of each peak was measured following background subtraction, assuming that a uniform background gradient under the peak connected the minima on either side. Intensity values (Fig. 3) were obtained after scaling between films in the stack, using peaks that were common to a pair of films and within the linear optical density range.

Factors affecting the accuracy of measurement of the peak positions were adventitious variations in the specimen-to-film distance and background noise on the film. The maximum errors in the estimate of lattice dimension due to these sources were, respectively, 0.25 Å (i.e., the value of 0.3%, above) and 0.2 Å (see Results). Thus the overall maximum error of measurement was ~0.3 Å, which is small compared with the observed changes in lattice dimension associated with the different treatments (Table I). Similar inferences apply to the observed changes in displacement of the (2,1) peak (Table II).

RESULTS

Design of Experiments

We considered that effects of variations between gap junction preparations (e.g., different lipid content or unequal

TABLE I

Effect of Dialysis Treatment on Lattice Dimension*

Dialysis treatment	Lattice dimension: Pellet (A)	Lattice dimension: Pellet (B)	Difference
	Å		
(a) EGTA‡ (A) vs. calcium§ (B)	82.09	81.47	−0.62
	81.80	80.09	−1.71
	82.96	80.87	−2.09
	82.66	80.07	−2.59
(b) Magnesium‖ (A) vs. calcium§ (B)	83.47	81.47	−2.00
	82.09	81.23	−0.86
(c) Calcium§ (A) vs. EGTA¶ (B)	81.00	81.77	+0.77
	80.79	81.55	+0.76
(d) Predialysis (A) vs. postdialysis** (B)	82.56	80.85	−1.71
	83.68	81.55	−2.13
	82.21	80.56	−1.55
	82.21	80.70	−1.51

* See Materials and Methods for details.
‡ 5 mM EGTA, 0.5 mM $MgCl_2$, 5 mM HEPES.
§ 0.05 mM $CaCl_2$, 5 mM HEPES.
‖ 0.25 mM $MgCl_2$, 0.1 mM EGTA, 5 mM HEPES.
¶ 0.05 mM $CaCl_2$, 5 mM HEPES, followed by 5 mM EGTA, 0.5 mM $MgCl_2$, 5 mM HEPES.
** 5 mM $NaHCO_3$ (containing ~0.05 mM Ca^{2+}; see text).

TABLE II

Effect of Dialysis Treatment on Displacement of the (2,1) Peak from the In-Plane Position

Dialysis treatment	Displacement of (2,1) peak: Pellet (A)	Pellet (B)	Difference
	$Å^{-1}$		
(a) EGTA (A) vs. calcium (B)*	0.00120	0.00090	−0.00030
	0.00115	0.00061	−0.00054
	0.00117	0.00082	−0.00035
	0.00104	0.00048	−0.00056
(b) Magnesium (A) vs. calcium (B)	0.00120	0.00075	−0.00045
	0.00103	0.00074	−0.00029
(c) Calcium (A) vs. EGTA (B)	0.00088	0.00104	+0.00016
	0.00064	0.00077	+0.00013
(d) Predialysis (A) vs. postdialysis (B)	0.00145	0.00071	−0.00074
	0.00179	0.00101	−0.00078
	0.00154	0.00077	−0.00077
	0.00174	0.00114	−0.00060

* See Table I for details; the order of experiments in Table I and Table II is the same.

amounts of impurities) might complicate interpretation of our findings. Therefore, our strategy throughout this investigation was to divide each preparation in two, subject the two halves to different treatments, and compare the x-ray patterns corresponding to those treatments. Pilot experiments demonstrated that results did not depend on the sequence in which these two patterns were recorded.

Features of the Low Angle Pattern

The low angle x-ray diffraction pattern from isolated mouse liver gap junctions has been described by Caspar et al. (1). In Fig. 1 we show analogous patterns from rat liver gap junctions, taken with our camera. The degree of orientation and quality was similar for pellets made from any given preparation, but between different preparations these features were more variable. Our findings mainly concern the positions and associated fine detail of the (1,0), (1,1), (2,0), and (2,1) arcs, centered on the equatorial (horizontal) plane. These arcs give information on the intensities along reciprocal lattice lines originating from ordered hexagonal lattices of connexons. The reciprocal lattice lines are not displayed directly, but are smeared into the arcs because of orientational disorder. The intensities on the (2,1) arc are in fact the overlapped contributions from both the (2,1) and (1,2) lattice lines.

Differences in the equatorial patterns due to different treatments were not easily detected by eye, but were clearly evident after circularly integrating along the arcs and plotting the summed optical densities as a function of reciprocal spacing (Fig. 2). In Fig. 2*a*, for example, the peaks shown in the upper plot (marked by vertical lines) lie at different positions from those of the lower plot, where the junctions have been subjected to a different treatment. In this example, the changes in position of the (1,0), (1,1), and (2,0) peaks corresponded to a change in lattice dimension of 1.71 Å. The broad (2,1) peak could not be simply correlated with lattice dimension because this peak contains strong contributions away from the equatorial plane (see below) and changes shape between treatments.

The distribution of intensities along the meridional (vertical) line consists of a series of broad arcs arising from the continuous diffraction perpendicular to the gap junction surface. With our samples, these intensities were often complicated by interference effects produced by the ordered stacking of groups of junctions (and sometimes membrane contaminants) within the pellet. The sharper interference arcs, in the more poorly oriented patterns, merged with the equatorial pattern, so that the intensity and position of the (1,0) arc was sometimes difficult to estimate.

Analysis of the Equatorial Peaks

We found that the (1,1) and (2,0) peaks were consistently the narrowest and most symmetrical, indicating that the corresponding reciprocal lattice lines contain the least significant contributions away from the equatorial plane. They were also less sensitive than the (1,0) peak to contamination by intensity from the meridian. Therefore, they provided the best

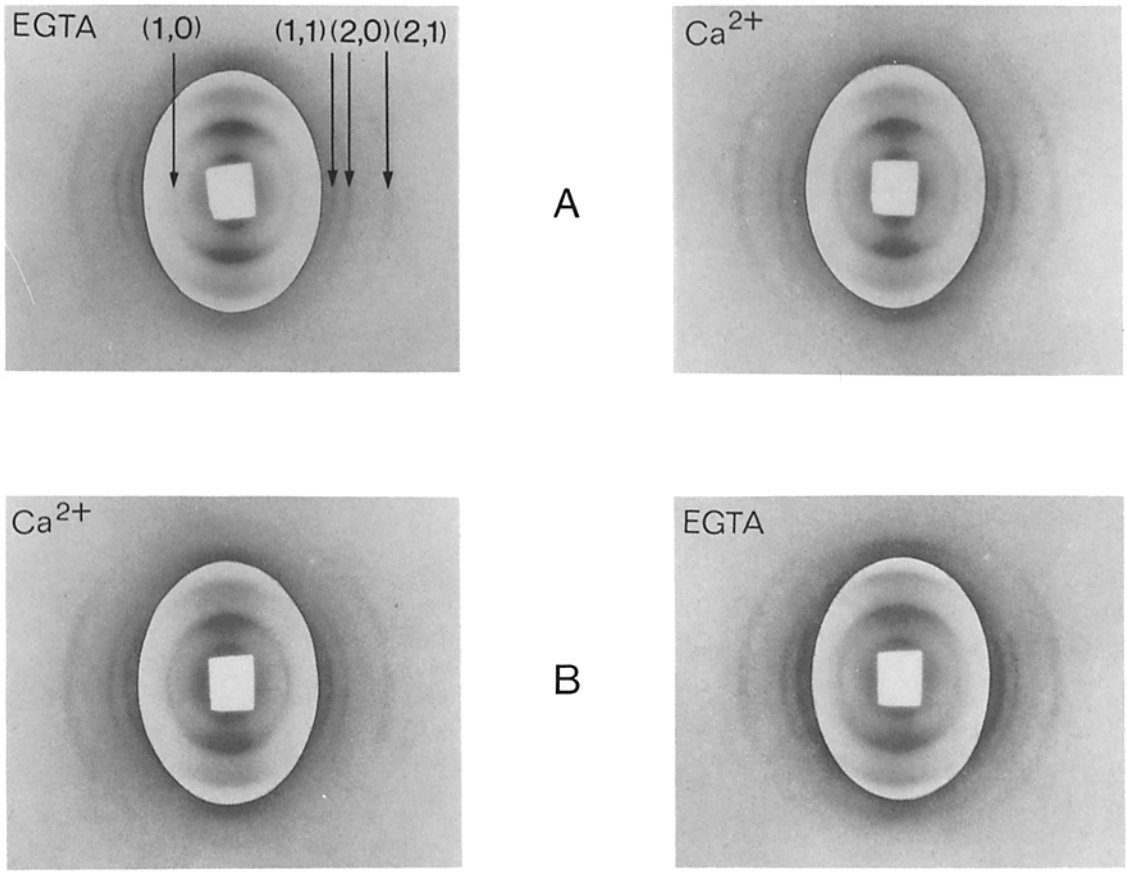

FIGURE 1 X-ray diffraction patterns of gap junctions from two different preparations, *A* and *B*. In *A* the junctions have been dialyzed against EGTA and against Ca^{2+}; in *B* the junctions have been dialyzed against Ca^{2+} in one case and against Ca^{2+} and then EGTA in the other. Solutions were the same as in Table I. The indices for the equatorial arcs are given in *A*. The central elliptical regions (from the third films back) mainly show detail along the meridian.

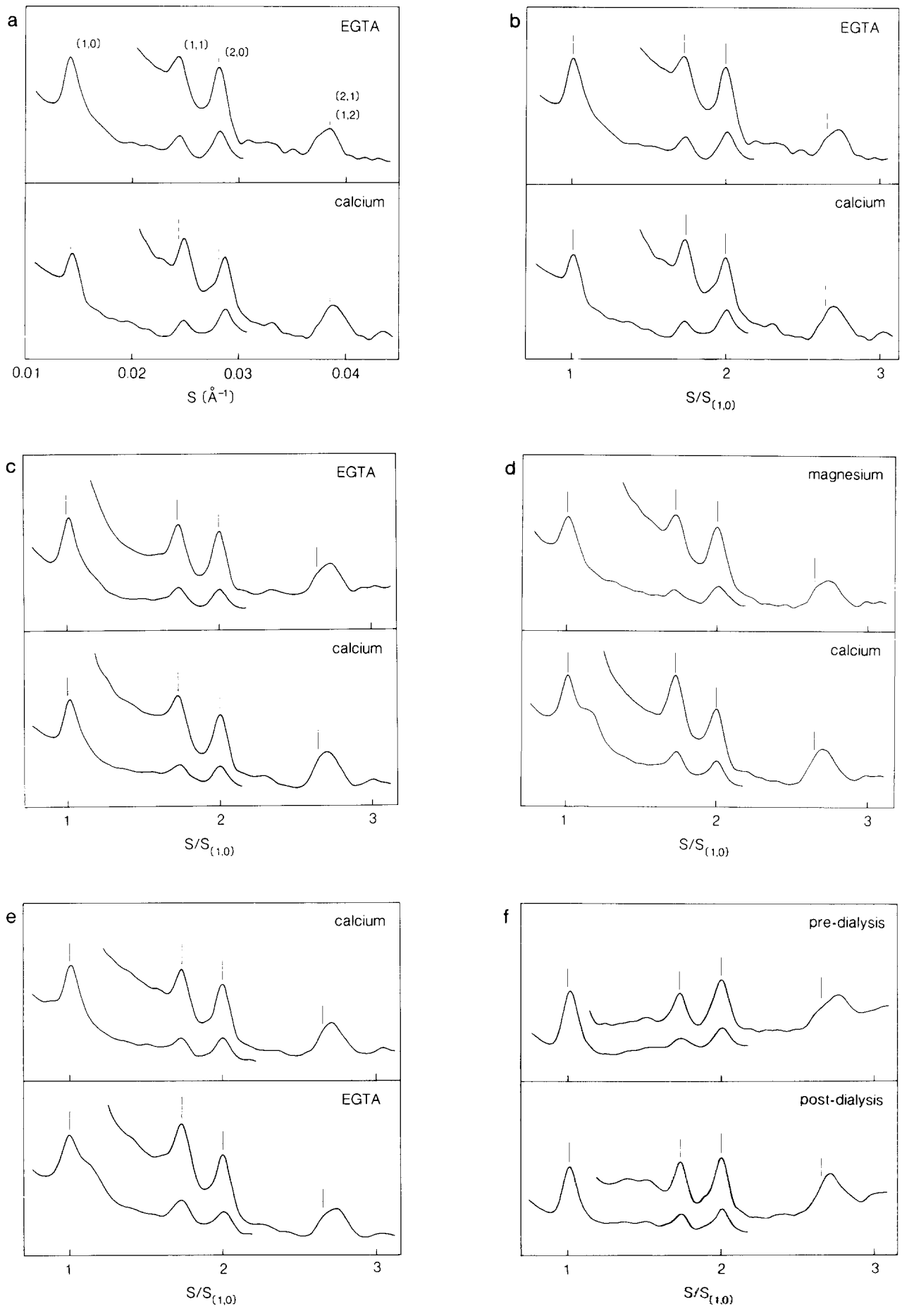

measurements for calculating the dimensions of the in-plane hexagonal lattice. In presenting the results below, we took the true reciprocal distance for the first order peak, $S_{(1,0)}$, to be an average derived from the measured values for the (1,1) and (2,0) peaks (i.e., $S_{(1,0)} = S_{(1,1)}/2\sqrt{3} + S_{(2,0)}/4$). We then took the figure of $2/\sqrt{3}\cdot S_{(1,0)}$ for the hexagonal lattice dimension. Alternative estimates of the hexagonal lattice dimension, using the (1,1) and (2,0) peaks independently, led to values that were consistently within 0.2 Å of each other.

The plots in Fig. 2, *b–f*, are constructed with the parameter $S/S_{(1,0)}$ as the abscissa so that changes in lattice dimension are not evident, but departures of peaks from their in-plane reciprocal lattice positions are emphasized. The in-plane reciprocal lattice positions for the (1,0), (1,1), (2,0), and (2,1) peaks are respectively 1, $\sqrt{3}$, 2, and $\sqrt{7}$ (marked by vertical lines). Both the (1,0) and (2,1) peaks are displaced from the calculated in-plane positions towards higher reciprocal spacings. The displacement of the (2,1) peak is the most marked and is a function of the treatment given (Table II). We conclude that this peak has strong intensities in regions away from the equatorial plane (7) and that these intensities vary according to the treatment given.

Effect of Calcium Ions

Equatorial patterns from preparations dialyzed against EGTA (i.e., Ca^{2+}-free) and Ca^{2+}-containing solutions were compared. The major changes accompanying exposure to 0.05 mM Ca^{2+} were found to be a decrease in lattice dimension by 1.75 Å (±0.72 SD; $n = 4$) (Table I *a*), a displacement of the (2,1) peak towards lower reciprocal spacing (Table II *a*, Fig. 2, *b* and *c*), and a decrease in the intensity of the (1,0) peak relative to the other three (Fig. 3 *a*).

Similar changes were observed in other experiments that used free Ca^{2+} concentrations ≥0.05 mM in the presence of EGTA, and also after the EGTA-treated pellets were washed with Ca^{2+}-containing solutions. On the other hand, junctions showed no sensitivity to the presence of Mg^{2+} at free concentrations as high as 0.16 mM (compare Table I, *a* and *b* and Table II, *a* and *b*; see also Fig. 2 *d*).

Small differences in the stacking properties of EGTA- and Ca^{2+}-treated gap junctions affect the detail along the meridian, so we were less successful in obtaining suitable comparisons from this part of the x-ray pattern. However, the predominant effect of Ca^{2+} in those comparisons that were feasible was to decrease the scale of the pattern in this direction (Fig. 4 *A*). The effect was demonstrated quantitatively in some cases by measuring the relative intensities and reciprocal positions of the maxima and minima along the meridian. We found that the relative intensities did not change by more than a few percent; however the positions of the maxima and minima, when plotted against each other on a linear scale, lay quite accurately on a straight line intersecting the origin (Fig. 5).

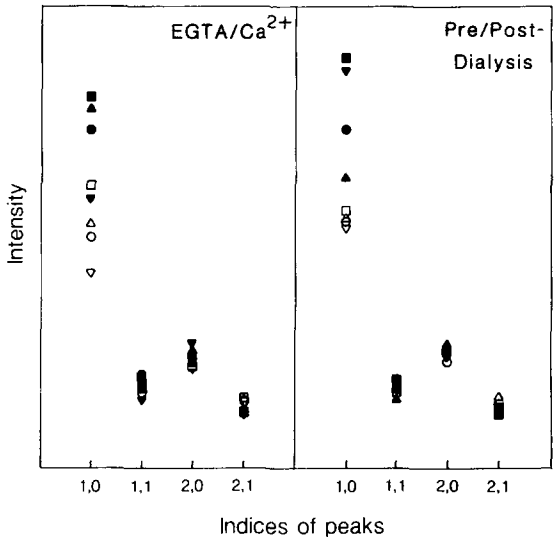

FIGURE 3 Intensities of equatorial arcs obtained after circular integration and background subtraction for (*a*) EGTA/Ca^{2+} and (*b*) pre-/postdialysis comparisons. Different symbols correspond to different preparations; solid symbols correspond to EGTA or predialysis treatments; open symbols correspond to Ca^{2+} or postdialysis treatments (see Table I for details). Intensities are peak values and have been scaled so that the sum of the values for the three outermost arcs is constant.

From the patterns in Fig. 4 *A* (and Fig. 1 *A*) the slope of this line, determined by a least square fit against the data points, was 1.039 (EGTA/Ca^{2+}), suggesting a linear increase in the dimension of the junction normal to the plane of the membranes of ~4% upon Ca^{2+} addition. This result may not apply to resolutions much higher than 32 Å, the limit of our measurements along the meridian.

Reversibility

To determine if the effects of Ca^{2+} on the x-ray pattern were reversible, we compared samples that had been dialyzed against Ca^{2+}-containing solutions (for 3 d) to those that had received this treatment and then been dialyzed against EGTA (for a further 3 d). We found small displacements of the (2,1) peak (Table II *c*, Fig. 2 *e*), together with small changes in lattice dimensions (Table I *c*); the sense of the differences were correlated with treatment as in the preceding section. Changes along the meridian were of the magnitude and sense described in the preceding section (Fig. 4 *B*, Fig. 5). Similar results, or no detectable change, were obtained by washing the Ca^{2+}-treated pellets with EGTA. Thus reversibility was difficult to achieve and sometimes appeared to be only partial, possibly because of some degradation associated with the long timescale over which these experiments were conducted.

FIGURE 2 Examples of optical density traces obtained by circularly integrating along the equatorial arcs of the x-ray patterns (using first two films in stack). The comparisons in *a–f* involve different treatments of gap junctions from the same preparations. The treatments are indicated for each trace, with solutions for *a*, *b*, and c as in Table I *a*, and *d*, *e*, and *f* as in Table I, *b*, *c*, and *d*, respectively. *a* and *b* are traces of the same data plotted in different ways: against the reciprocal spacing, *S*, in *a* to emphasize the changes in position of the (1,0), (1,1), and (2,0) peaks; and against $S/S_{(1,0)}$ in *b* to emphasize the change in position of the (2,1) peak. The vertical (dashed) lines in *a* mark the positions of the peaks in the EGTA-treated junctions; the vertical lines on the remaining traces mark the estimated in-plane hexagonal lattice positions (at 1, $\sqrt{3}$, 2, and $\sqrt{7}$). The traces in c are from the pattern in Fig. 1 *A*; the traces in e are from the pattern in Fig. 1 *B*. The shoulder associated with some of the (1,0) peaks is due to contamination from the meridian.

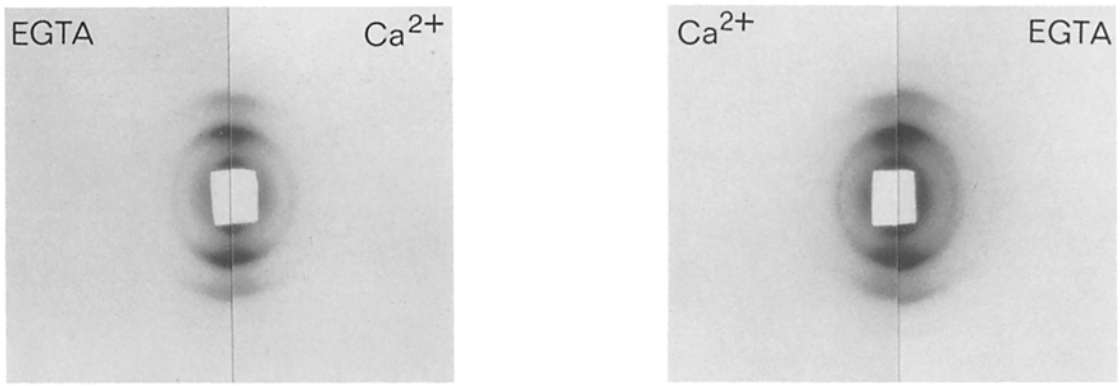

FIGURE 4 Comparison of the meridional patterns of Fig. 1, showing small changes in the positions of the arcs associated with EGTA/Ca^{2+} and Ca^{2+}/EGTA treatments. The two patterns in *A* correspond to those in Fig. 1 *A*; the two patterns in *B* correspond to those in Fig. 1 *B*.

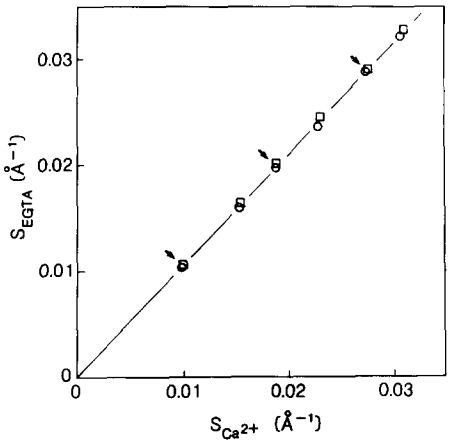

FIGURE 5 Reciprocal positions of maximum and minimum (arrows) intensities along the meridians shown in Fig. 4 (and Fig. 1). Positions for the EGTA-treated junctions are plotted against those for the Ca^{2+}-treated junctions. Circles correspond to the patterns in Fig. 4 *A*; squares correspond to the patterns in Fig. 4 *B*.

Effect of pH

Several comparisons were carried out on EGTA-treated pellets, using different pHs in the range 6.0–8.0. No changes were detected in either the equatorial or meridional regions of the x-ray patterns (data not shown).

Correlation with Previous Findings

Previous electron microscopy studies showed that dialysis of freshly isolated junctions against bicarbonate buffer at pH 8.0 brought about a structural change involving a rearrangement of the connexon subunits (14, 15). We investigated x-ray patterns from junctions given those treatments and obtained results that were similar to those of the EGTA/Ca^{2+} experiments above. After dialysis against the bicarbonate buffer, the lattice dimension was 1.75 Å (±0.25 SD; $n = 4$) less than it was beforehand (Table I*d*), the (2,1) peak was displaced towards lower reciprocal spacing (Table II*d*, Fig. 2*f*), and the intensity of the (1,0) peak had decreased (Fig. 3*b*). The displacement of the (2,1) peak was significantly larger than in the above experiments, suggesting that the structures of the EGTA-treated and predialysis junctions may not be quite identical. On the other hand, all the data suggest that the Ca^{2+}-treated and postdialysis junctions are equivalent.

At the time of these experiments, no precautions were taken to eliminate trace amounts of Ca^{2+} from the dialysis solution since its possible significance at such low concentrations was not suspected. However, subsequent measurements of Ca^{2+} present using the dye, Arsenazo III, indicated that the levels were between 0.01 and 0.1 mM, i.e., approximately the same concentration as we used in the EGTA/Ca^{2+} experiments above. Thus the equivalence of the x-ray patterns from Ca^{2+}-treated and postdialysis junctions seems merely to reflect the presence of Ca^{2+} in either case.

DISCUSSION

We found that rat liver gap junctions isolated in Ca^{2+}-free media (15; see Materials and Methods) change their structure when placed in an environment containing Ca^{2+}. Calcium ions are known to have physiological significance and it is therefore of interest to consider the chemical characteristics of this response and the nature of the structural changes involved.

Calcium Sensitivity

The experiments showed that the junctions were sensitive to Ca^{2+} levels as low as 0.05 mM and that the structural responses to this ion were reversed when it was removed. Specificity of the effect was demonstrated to the extent that x-ray patterns from junctions in relatively high concentrations of Mg^{2+} were the same as those obtained with Ca^{2+}-free media. pH, which also affects the junctional permeability in whole cells, had no influence under the very limited set of conditions tried; neither did the different buffers used.

Sensitivity of gap junction channels to closure by Ca^{2+} has been estimated by several kinds of measurements made on whole cells, and response thresholds in the region of 0.05–0.10 mM have been reported (10, 11). Actual values probably depend on the system being investigated and may also be affected by the circumstances. For example, sensitivity could be modified upon isolation, by loss of peripheral membrane proteins or of cytoplasmic molecules (5), or by the reduction in ionic strength. Given the present limited characterization, it cannot be proven that Ca^{2+} is stimulating the same structural response in the isolated material as it is in whole cells. The observed chemical parallels do however make this a reasonable possibility.

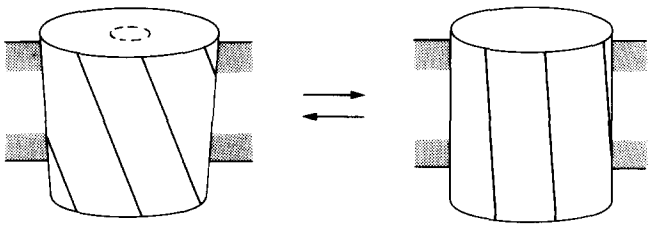

FIGURE 6 Schematic picture (not to scale) of the two connexon subunit configurations suggested by these x-ray experiments and previously (14). The $-Ca^{2+}$ configuration is on the left and the $+Ca^{2+}$ configuration is on the right. On exposure to Ca^{2+} the subunits appear to align more nearly parallel to the channel, thereby increasing slightly the length of the connexon and decreasing slightly its maximum dimension parallel to the plane of the membrane. The dimensional changes could not be measured accurately in the earlier study.

Structural Interpretation

The major Ca^{2+}-mediated responses observed in the x-ray patterns were reductions in the intensity of the (1,0) peak and in the off-equatorial contributions to the (2,1) peak, and changes of scale equivalent to a decrease in lattice dimension, but an increase in the dimension perpendicular to the lattice. These responses were also produced by dialysis of freshly isolated junctions against a low salt solution, the treatment given previously to produce a structural change (14, 15).

In the earlier study, the structural change was analyzed in three dimensions by electron microscopy using negative stain. It was found to involve a coordinated rearrangement of the connexon subunits about their central (hexad) axis. Before dialysis they were strongly inclined tangentially around the channel, whereas afterwards they were aligned more nearly parallel to the channel and closer together near the cytoplasmic face (Fig. 6).

The correspondence between the two configurations found by electron microscopy and the ones indicated by these x-ray results can be examined by comparing the two sets of diffraction data (Fig. 2 in reference 14). With both techniques the dialysis leads to: (*a*) a reduction in the integrated intensity of the (1,0) peak by ~20% compared with very small changes in the integrated intensities of the (1,1) and (2,0) peaks; and (*b*) a weakening of the off-equatorial contributions to the (2,1) peak by a substantial amount compared with changes of the same nature to the other three peaks. This matching of intensity changes between the two sets of data is striking considering that negative stain gives an incomplete picture of the detail within the membrane, and provides strong evidence that the structural change in solution produced by the dialysis is essentially the one found by electron microscopy. The same argument must apply for the Ca^{2+}-mediated change, since the dialysis treatment and addition of Ca^{2+} affect the x-ray pattern in equivalent ways. Therefore, a minimal conclusion from this comparison is that the connexon subunits are first inclined tangentially to the channel and then align more nearly parallel to it when Ca^{2+} is added. This conclusion may also be reached independently by considering the changes in displacement of the (2,1) peaks from the calculated in-plane positions (Table II). Model calculations show that these changes are a sensitive function of changes in subunit tilt.

With the subunits aligned more nearly parallel to the channel, the connexon should become slightly longer and more radially compact (Fig. 6). Thus the dimensional changes one would expect to detect as a result of this rearrangement are small increases and small decreases, respectively, in the extent of the structure perpendicular and parallel to the membranes. We observed increases and decreases of ~4 and ~2% in these two directions, which are reasonable values, assuming that there are small inclination changes of the subunits.

A more quantitative evaluation of the rearrangement than this cannot be made from the data presented. There are complications that would be revealed by a more detailed structure analysis. For example, the tightness of packing of oppositely facing pairs of connexons would be affected by the rearrangement, adding a further dimensional component normal to the membranes. The nature of the lateral packing of neighboring connexons is also important. Connexons can pack more closely laterally, by interlocking, when their subunits are more nearly normal to the plane of the membrane (and hence more nearly parallel to those of neighboring connexons) than when they are tilted. Since the different configurations would require variability in the amount of lipid filling the intervening spaces, restriction of the lipid present in isolated junctions may exert constraints on changes, possibly leading to some distortion of the structure.

Relation to Other X-ray Studies

Caspar, Makowski and co-workers (1, 7, 8) compared x-ray patterns from mouse liver junctions isolated by several alternative methods. The structural changes they described are different from the ones described here. In our case, the dimensional change perpendicular to the plane of the membranes compensated for the dimensional changes in this plane so that the volume of the "unit cell" remained approximately constant; in their case, the dimensional changes found were of the same sense in all directions. Thus they were investigating a different phenomenon.

CONCLUSION

The structure of the connexon in isolated rat liver gap junctions is sensitive to low Ca^{2+} concentrations. A simple interpretation of the observed responses is that the connexon subunits become aligned more nearly parallel to the channel on exposure to Ca^{2+}, thereby making the connexon itself slightly longer and more radially compact. This rearrangement may be part of a coordinated mechanism by which the channel closes.

We are particularly grateful to Tony Woollard and Chris Raeburn (Medical Research Council, Laboratory of Molecular Biology, Cambridge, England) for constructing the x-ray camera, to David Austen and David Grano (Stanford University) for providing computer programs, and to Guido Zampighi for helpful discussions.

The research was supported by grants GM27764, GM28668, and GM30387 from the National Institutes of Health.

Received for publication 18 April 1983, and in revised form 25 July 1983.

REFERENCES

1. Caspar, D. L. D., D. A. Goodenough, L. Makowski, and W. C. Phillips. 1977. Gap junction structures. I. Correlated electron microscopy and x-ray diffraction. *J. Cell Biol.* 74:605–628.
2. Goodenough, D. A. 1976. In vitro formation of gap junction vesicles. *J. Cell Biol.* 68:220–231.
3. Harris, A. L., D. C. Spray, and M. V. L. Bennett. 1981. Kinetic properties of a voltage-dependent junctional conductance. *J. Gen. Physiol.* 77:95–117.

4. Hertzberg, E. G., T. S. Lawrence, and N. B. Gilula. 1981. Gap junctional communication. *Annu. Rev. Physiol.* 43:479–491.
5. Johnston, M. F., and F. Ramon. 1981. Electrotonic coupling in internally perfused crayfish segmented axons. *J. Physiol. (Lond.).* 317:509–518.
6. Loewenstein, W. R. 1981. Junctional intercellular communication: the cell-to-cell membrane channel. *Physiol. Rev.* 61:829–913.
7. Makowski, L., D. L. D. Caspar, W. C. Phillips, and D. A. Goodenough. 1977. Gap junction structures. II. Analysis of the x-ray diffraction data. *J. Cell Biol.* 74:629–645.
8. Makowski, L., D. L. D. Caspar, D. A. Goodenough, and W. C. Phillips. 1982. Gap junction structures. III. The effect of variations in the isolation procedure. *Biophys. J.* 37:189–191.
9. Obaid, A. L., S. J. Socolar, and B. Rose. 1983. Cell-to-cell channels with two independently regulated gates in series. *J. Membr. Biol.* 73:69–89.
10. Rose, B., and W. R. Loewenstein. 1975. Permeability of cell junction depends on local cytoplasmic calcium activity. *Nature (Lond.).* 254:250–252.
11. Spray, D. C., J. H. Stern, A. L. Harris, and M. V. L. Bennett. 1981. Gap junctional conductance: comparison of sensitivities to H and Ca ions. *Proc. Natl. Acad. Sci. USA.* 79:441–445.
12. Thomas, M. V., and A. L. F. Gorman. 1977. Internal calcium changes in a bursting pacemaker neuron measured with Arsenazo III. *Science (Wash. DC).* 196:531–533.
13. Turin, L., and A. Warner. 1980. Intracellular pH in early *Xenopus* embryos: its effect on current flow between blastomeres. *J. Physiol. (Lond.).* 300:489–505.
14. Unwin, P. N. T., and G. Zampighi. 1980. Structure of the junction between communicating cells. *Nature (Lond.).* 283:545–549.
15. Zampighi, G., and P. N. T. Unwin. 1979. Two forms of isolated gap junctions. *J. Mol. Biol.* 135:451–464.